Mercury inputs to Great Salt Lake, Utah: Reconnaissance-Phase results

David Naftz
US Geological Survey, Salt Lake City, UT

Christopher Fuller
US Geological Survey, Menlo Park, CA

Jay Cederberg
US Geological Survey, Salt Lake City, UT

David Krabbenhoft
US Geological Survey, Middleton, WI

John Whitehead
Utah Division of Water Quality, Salt Lake City

See next page for additional authors

Follow this and additional works at: https://digitalcommons.usu.edu/nrei

Utah State University
MERRILL-CAZIER LIBRARY

Mercury inputs to Great Salt Lake, Utah: Reconnaissance-Phase results

Authors

David Naftz, Christopher Fuller, Jay Cederberg, David Krabbenhoft, John Whitehead, Jodi Garberg, and Kimberly Beisner

Mercury Inputs to Great Salt Lake, Utah: Reconnaissance-Phase Results

David Naftz[1], Christopher Fuller[2], Jay Cederberg[1], David Krabbenhoft[3], John Whitehead[4], Jodi Garberg[4] & Kimberly Beisner[1]

[1]U.S. Geological Survey, Salt Lake City, Utah, USA, [2]U.S. Geological Survey, Menlo Park, California, USA, [3]U.S. Geological Survey, Middleton, Wisconsin, USA, [4]Utah Division of Water Quality Division, Salt Lake City, Utah, USA

Corresponding author:
David Naftz
USGS, 2329 W. Orton Circle, Salt Lake City, Utah 84119, USA
E-mail: dlnaftz@usgs.gov

ABSTRACT

In response to increasing public concern regarding mercury (Hg) cycling in Great Salt Lake (GSL) ecosystem, a series of studies were initiated to differentiate between the mass of Hg from riverine versus atmospheric sources to GSL. Cumulative riverine Hg load to GSL during a 1 year time period (April 1, 2007 to March 31, 2008) was 6 kg, with almost 50% of the cumulative Hg load contributed by outflow from Farmington Bay. Comparison of cumulative annual atmospheric Hg deposition (32 kg) to annual riverine deposition (6 kg) indicates that atmospheric deposition is the dominant input source to GSL. A sediment core collected from the southern arm of GSL was used to reconstruct annual Hg deposition rates over the past ~ 100 years. Unlike most freshwater lakes, small changes in water level in GSL significantly changes the lake surface area available for direct deposition of atmospheric Hg. There is good agreement between lake elevation (and corresponding lake surface area) and Hg deposition rates estimated from the sediment core. Higher lake levels, combined with sediment focusing processes, result in an increase in Hg accumulation rates observed in the sediment core. These same combination of processes are responsible for the lower Hg accumulation rates observed in the sediment core during historic low stands of GSL.

INTRODUCTION

Great Salt Lake (GSL), in the western United States, is a terminal lake with a surface area that can exceed 5100 km^2 (Figure 1). The lake is bordered on the west by desert and on the east by the Wasatch Mountain Range. Completion of a railroad causeway in 1959 divided GSL into a North and South Arm (Figure 1) and significantly changed the water and salt balance (Loving et al. 2000). More than 95% of the freshwater surface inflows enter GSL south of the railroad causeway resulting in consistently higher salinities in lake water north of the railroad causeway. A similar rock-filled automobile causeway separates Farmington Bay from the main body of GSL (Figure 1).
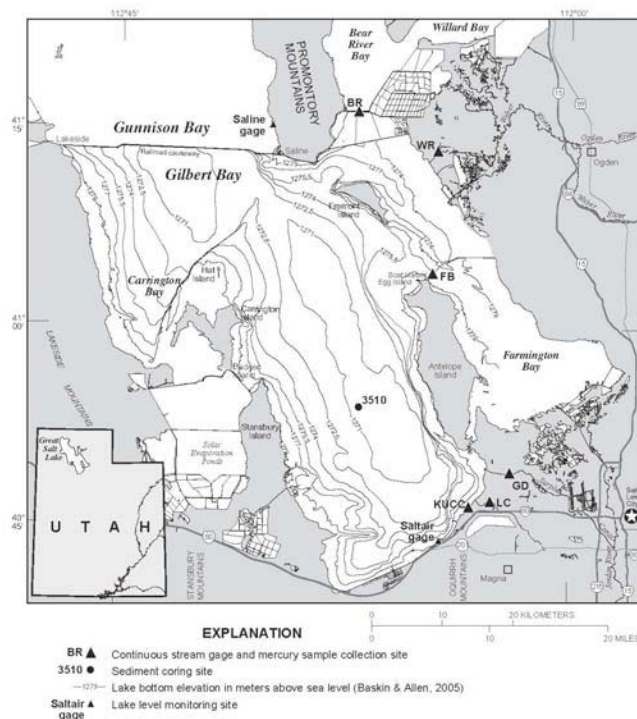
Figure 1–Location of stream gages, lake elevation monitoring sites, and sediment core site, Great Salt Lake, Utah.

The GSL ecosystem receives industrial, urban, mining and agricultural discharge from a 3.8 x 10^4 km^2 watershed with a population exceeding 1.7 million people. The open water and adjacent wetlands of the GSL ecosystem support millions of migratory waterfowl and shorebirds from throughout the Western Hemisphere (Aldrich & Paul 2002). In addition to supporting migratory dependent waterbirds, the brine shrimp population residing in GSL supports a shrimp industry with annual revenues as high as 60 million US dollars (Isaacson et al. 2002). Other industries supported by GSL include mineral production (halite, K salts, Mg metal, Cl_2, $MgCl_2$, and nutritional supplements) and recreation that includes waterfowl hunting (Anderson & Anderson 2002; Butts 2002; Isaacson et al. 2002; Tripp 2002).

Despite the ecological and economic importance of GSL, little is known about the input and biogeochemical cycling of Hg in the lake and how increasing anthropogenic pressures may affect its cycling. Reconnaissance-phase sampling and analysis of water samples from GSL by the

U.S. Geological Survey (USGS) from 2003 to 2007 found elevated (median concentration = 24 ng/l) concentrations of methyl Hg (CH_3Hg) (Naftz et al. 2006, 2008). In response to elevated CH_3Hg levels in water samples from GSL, the State of Utah collected and analyzed breast tissue for total Hg from seven duck species that utilized GSL and surrounding wetlands (Utah Department of Health 2005). These reconnaissance-phase analyses found that a number of the breast muscle samples exceeded the U.S. Environmental Protection Agency (USEPA) screening level of 0.3 mg/kg Hg (wet weight), the concentration at which limited human consumption of bird breast muscle is recommended (USEPA 2000). As a result of the reconnaissance-phase Hg assessment of the duck population in GSL, a health advisory was issued by the Utah Department of Health in September 2005 warning against unlimited human consumption of Northern Shoveler and Common Goldeneye ducks harvested from GSL.

Additional investigations into Hg cycling in GSL by the USGS (Naftz et al. 2008) found that separation of GSL into two distinct hydrologic and geochemical systems from the construction of a railroad causeway in the late 1950s created a persistent and widespread anoxic layer in the southern part of GSL. This anoxic layer, referred to as the deep brine layer (DBL), has high rates of SO_4 reduction, likely increasing the Hg methylation potential. High concentrations of CH_3Hg (median concentration = 24 ng/l, n = 15) in whole-water samples were found in the DBL with a significant proportion (31–60%) of total Hg in the CH_3Hg form. Furthermore, Naftz et al. (2008) used hydroacoustic and sediment-trap data to show that turbulence introduced by internal waves generated during sustained wind events can temporarily mix the elevated CH_3Hg concentrations in the DBL with the more biologically active upper brine layer (UBL).

In response to increasing public concern regarding Hg input to the GSL ecosystem and to begin to consider possible remediation alternatives, the Utah Department of Environmental Quality (UDEQ) and USGS initiated additional studies to differentiate the relative amounts of Hg from riverine versus atmospheric sources to GSL. Specific objectives of this study were to (1) accurately measure stream discharge and whole-water Hg concentration at all major inflow sites to GSL; (2) utilize data collected in objective one in combination with regression modeling techniques to determine daily and annual Hg loads to GSL; and (3) utilize sediment-core data collected from GSL to reconstruct riverine and atmospheric Hg input to GSL over the last 100 years. This chapter presents the results related to these objectives.

METHODOLOGY

Field Methods

Stream discharge at the Goggin Drain (GD), Weber River (WR), and Lee Creek (LC) gages (Figure 1) was measured using standard USGS methods (Buchanan & Somers 1968, 1969; Carter & Davidian 1968) using a continuous record of water stage calibrated to periodic measurements of streamflow. Due to the low channel gradients and wind influence on inflow rates at the Bear River (BR), Farmington Bay (FB), and Kennecott Utah Copper Corporation (KUCC) gage sites (Figure 1), normal stage-to-discharge relationships did not exist. Instead, hydroacoustic instrumentation in combination with velocity index methods (Simpson 2001) was used to accurately gage streamflow at those sites. Discharge from FB enters into GSL via an opening in the rock-filled causeway that artificially separates Farmington Bay from the main body of GSL (Figure 1).

During the study period (April 1, 2007 to March 31, 2008), whole-water samples from the six inflow sites were collected at the centroid of flow directly into pre-cleaned Teflon bottles provided by the U.S. Geological Survey Mercury Research Laboratory in Middleton, Wisconsin. Sample bottles were double bagged during storage and shipping. Because of the low-gradient conditions at selected inflow sites, the direction of inflow was noted during sample collection. Within 8 hours after collection, water samples were acidified with ultra-pure, 50% HCl in a fully enclosed processing chamber to prevent the introduction of airborne Hg to the water samples. During sample collection, personnel wore arm-length, powder-free gloves to minimize sample contamination. The sediment core from the top 0.5 m of sediment underlying GSL was collected using a box-coring device (Van Metre et al. 2004) suspended from a davit attached to the USGS Research vessel D. Stephens. After collection, the core was chilled to $4^{\circ}C$ during transport to shore for processing. Once on shore (< 8 hours after core collection), the top 10 cm section of the sediment core was sliced into 1 cm intervals and transferred into 200 ml, wide-mouthed plastic containers and frozen until the samples could be freeze dried prior to chemical analysis. Weights of sediments before and after drying were recorded for determining bulk density, ρ (g dry sediment per cm^3 wet sediment). Particle dry density, ρ_b and salt content were determined by measuring displacement of dry sediment added to deionized water in volumetric flasks and resulting dissolved salt concentration. Sediment porosity (φ) was determined from weight loss on drying sediment samples and ρ_b with correction for salt contribution to dry sediment weight following the method described in Van Metre et al. (2004). The total dry sediment

38

mass (corrected for salt content) in each interval in g/cm^2 was calculated by multiplying the dry sediment porosity (1-φ, cm^3) by ρ_b (g/cm^3) and the thickness for each interval thickness, and summing over the length of the core from the surface downward.

Laboratory Methods

All water analyses were performed at the USGS Hg Research Laboratory in Middleton, Wisconsin. Total Hg (Hg$_t$) in whole-water samples was determined using cold vapor atomic fluorescence spectrometry (CVAFS) (Olson & DeWild 1999). The CH$_3$Hg in whole-water samples was determined using distillation/ethylation/gas-phase separation with CVAFS detection (DeWild et al. 2002). Primary standards for Hg$_t$ were obtained commercially and certified against a NIST standard reference material. No reference materials are currently available for CH$_3$Hg. Standards for CH$_3$Hg were prepared in the laboratory. Known reference samples were analyzed at the beginning of each analytical run, after every 10 samples and at the end of each run. Method blanks were prepared by adding SnCl$_2$ to 125 ml of Hg-free water and purging for 20 minutes to ensure removal of any residual Hg. Method blanks were run periodically during each sample run and used to calculate the daily detection limit (DDL). The accepted value for the DDL is < 0.04 ng/l. Matrix spikes were analyzed during each run or every 10 samples. Percent recovery of matrix spikes had to fall between 90% and 110% for the sample run to be accepted. Three field replicates and two process blanks were collected and analyzed for Hg$_t$ and CH$_3$Hg. Field replicate results were in close agreement, with replicates ranging from 3.0% to 5.5% for Hg$_t$ and 2.7% to 15.9% of the routine sample value for CH$_3$Hg. Process blanks had low Hg$_t$ (0.08 and 0.10 ng/l) and CH$_3$Hg (< 0.04 ng/l) concentrations. Additional details on Hg laboratory methods and quality assurance and quality control procedures can be found at http://infotrek.er.usgs .gov/mercury/.

The Hg$_t$ in sediment samples was extracted and analyzed according to the methods outlined in Olund et al. (2004). Each sediment sample was extracted by room-temperature acid digestion and oxidation with aqua regia. The samples were then brought up to volume with a 5% BrCl solution to ensure complete oxidation and then heated at 50°C in an oven overnight. Samples were then analyzed for Hg$_t$ with an automated flow injection system incorporating a cold vapor atomic fluorescence spectrometer. A method detection limit of 0.3 ng of Hg per digestion bomb was established using multiple analyses of a solid-phase environmental sample. Based on the range of masses processed, the minimum sample reporting limit for this method varied from 0.6 to 6 ng/g.

Activities of ^{210}Pb, ^{226}Ra, and ^{7}Be were measured simultaneously in freeze-dried sections of the sediment core by gamma spectrometry (Fuller et al. 1999; Van Metre et al. 2006). Subsamples of dried sediment samples were sealed in 7 ml scintillation vials and counted using a high resolution intrinsic germanium well detector. The upper 3 cm of the core were counted within two weeks of collection for determining ^{7}Be (half life 53 days) as an indicator of recent sediment deposition and reworking by mixing or resuspension processes. ^{210}Pb was determined from the 46 keV gamma emission line correcting for sample self absorption following the method of Cutshall et al. (1983). The supported ^{210}Pb activity, defined by its long-lived progenitor, ^{226}Ra activity, was determined on each interval from the 352 keV and 609 keV gamma emission lines of ^{214}Pb and ^{214}Bi daughters of ^{226}Ra, respectively. Self absorption of the ^{214}Pb, ^{214}Bi, and 474 keV ^{7}Be gamma emission lines was negligible. The difference between ^{210}Pb and ^{226}Ra is defined as unsupported or excess ^{210}Pb (^{210}Pb$_{XS}$). Detector efficiency for each isotope was determined from NIST traceable standards. NIST and IAEA reference materials were used to check detector calibration. The reported uncertainty in the measured activity was calculated from the random counting error of samples and background spectra at the one standard deviation level was typically within ±10%. The measured activities of replicate analysis of material from the same interval agreed to within ± 15%.

Mass Loading Estimation Method

The USGS loading software, LOADEST (Runkel et al. 2004), was used to estimate the mass loading of whole water Hg$_t$ and whole water CH$_3$Hg at each gage site. The automated model selection in LOADEST was used to select the best regression model from the set of nine predefined models (Table 1). Under the automated selection option, adjusted maximum likelihood estimation (AMLE) (Cohn 1988; Cohn et al. 1992) is used to determine model coefficients and estimates of log load. The predefined model with the lowest value of the Akaike Information Criterion (AIC) statistic was then used for final load estimation (Judge et al. 1988).

RESULTS AND DISCUSSION

Simulation of Hg Loadings from Inflow Sites

The LOADEST software requires a minimum of 12 water quality samples to model chemical loadings. Currently (May 2008), only seven Hg$_t$ and CH$_3$Hg samples have been collected at each of the six inflow sites. To account for the sample deficit, synthetic water-quality samples were input to the LOADEST calibration files during a similar time

period (± 7 days) and flow regime (± 10%) as the actual water-quality samples that were collected. Although the insertion of synthetic values into the LOADEST calibration file weakens the annual loading simulation for each input site, this approach allows for a preliminary estimate of annual, riverine Hg_t and CH_3Hg loads to GSL. Future water-quality sampling will allow for the replacement of synthetic water-quality samples with actual samples in the LOADEST calibration file, thereby providing refined annual estimates of Hg loads (dissolved + particulate). Additional water-quality samples collected during varying hydrologic conditions, including peak discharge events, will further improve the annual Hg loading estimates. Details of LOADEST model calibration results are provided for each inflow site.

Because of the low-gradient conditions associated with the Bear River Bay and Farmington Bay outflow sites, wind events can temporarily reverse the normal direction of flow into GSL. When reverse flow conditions were recorded, a near zero (< 0.0001 m^3/s) discharge was used in the LOADEST calibration files.

Lee Creek near Magna, Utah: The LOADEST model calibration file contained seven observations for Hg_t and CH_3Hg during the time period of April 2007 through March 2008 (Figure 2). The LOADEST estimation file contained 397 measurements of mean daily discharge ranging from 0.8 to 3.6 m^3/s during the time period from March 2007 through March 2008. Regression model 9 (Table 1) was found to best simulate daily Hg_t loads (R^2 = 0.9717) and CH_3Hg loads (R^2 = 0.9718) from Lee Creek to GSL.

Comparisons between the measured and simulated loads of Hg_t at the Lee Creek gage indicate good agreement (Figure 2). The difference between measured and simulated Hg loads ranged from -4.5 to +6.1% for Hg_t and -23.7 to +10.4% for CH_3Hg loads. Annual load from Lee Creek to GSL during the monitoring period was 0.30 kg for Hg_t (Figure 3) and 9.2 g for CH_3Hg.

Goggin Drain near Magna, Utah: The LOADEST model calibration file contained seven observations for Hg_t and CH_3Hg during the time period of April 2007 through March 2008 (Figure 4). The LOADEST estimation file contained 397 measurements of mean daily discharge ranging from 0.2 to 30.9 m^3/s during the time period from March 2007 through March 2008. Regression model 9 (Table 1) was determined to best simulate daily Hg_t loads (R^2 = 0.9998) and CH_3Hg loads (R^2 = 0.9995) from Goggin Drain to GSL.
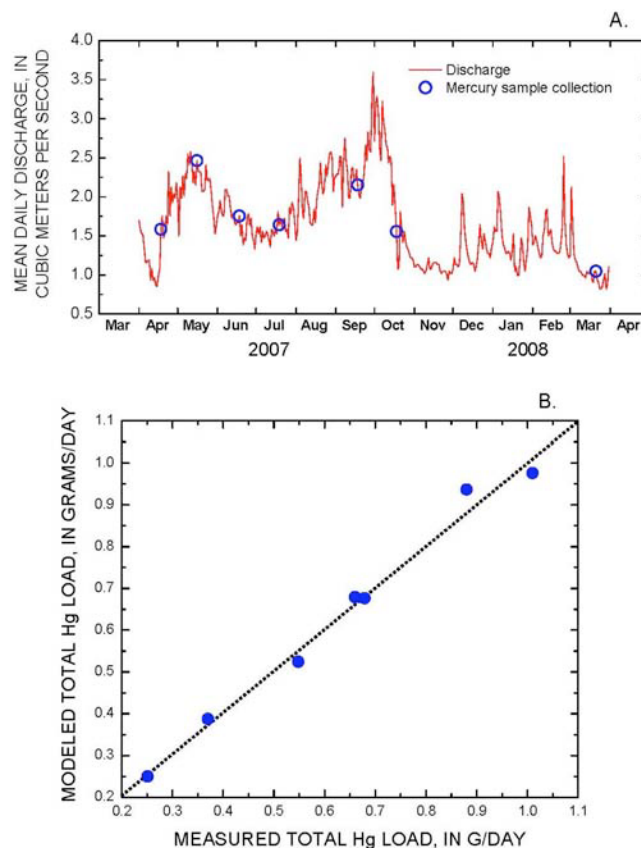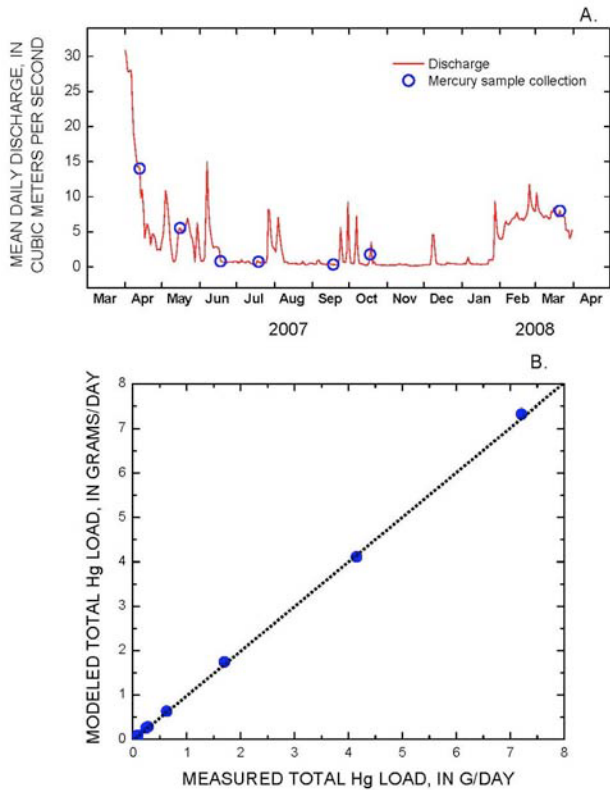

Figure 2–Stream discharge and dates when mercury samples were collected at the Lee Creek gaging station (A) and comparison between measured and modeled total mercury loads (B). Dashed line indicates one-to-one correspondence between measured and modeled mercury loads.
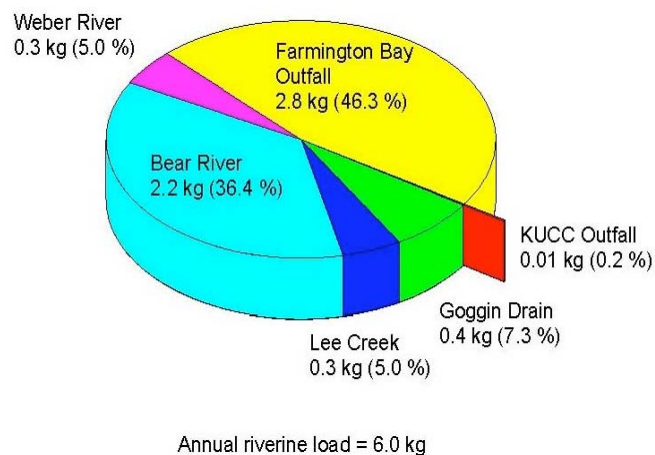
Figure 3–Distribution of Hg_t (dissolved + particulate) loads contributed to Great Salt Lake from each inflow site during April 1, 2007 to March 31, 2008. KUCC is the abbreviation for Kennecott Utah Copper Corporation.
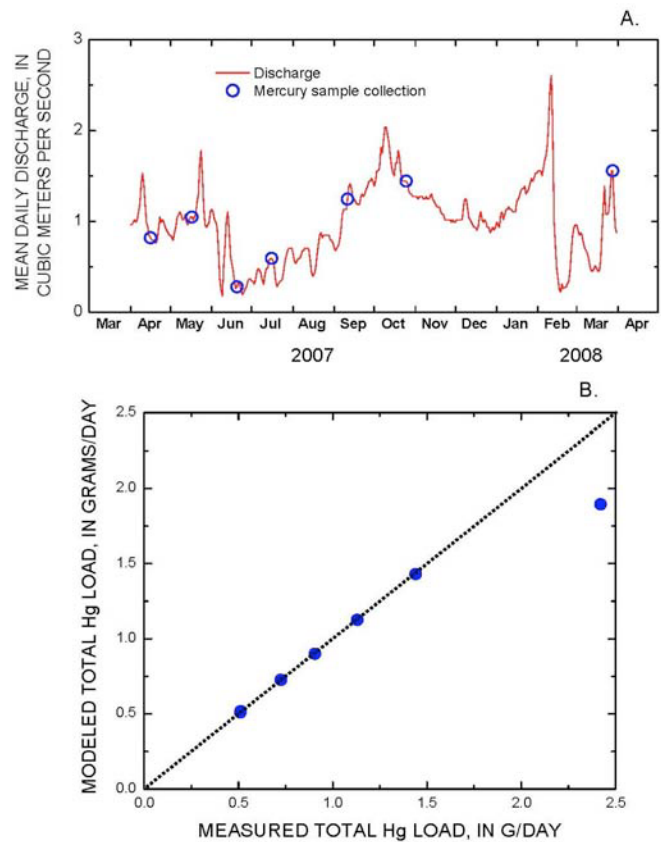
Figure 4–Stream discharge and dates when mercury samples were collected at the Goggin Drain gaging station (A) and comparison between measured and modeled total mercury loads (B). Dashed line indicates one-to-one correspondence between measured and modeled mercury loads.

Comparisons between the measured and simulated loads of Hg_t at the Goggin Drain gage indicate good agreement (Figure 4). The difference between measured and simulated Hg loads ranged from -1.1 to +2.8% for Hg_t and -2.9 to +6.0% for CH_3Hg loads. Annual load from Goggin Drain to GSL during the monitoring period was 0.44 kg of Hg_t (Figure 3) and 13 g of CH_3Hg.

Weber River near West Warren, Utah: The LOADEST model calibration file contained seven observations for Hg_t and CH_3Hg during the time period of April 2007 through March 2008 (Figure 5). The LOADEST estimation file contained 397 measurements of mean daily discharge ranging from 0.2 to 2.6 m^3/s during the time period from March 2007 through March 2008. Regression model 9 (Table 1) was determined to best simulate daily Hg_t loads ($R^2 = 0.9987$) and CH_3Hg loads ($R^2 = 0.9964$) from Weber River to GSL.

Comparisons between the measured and simulated loads of Hg_t at the Weber River gage indicate good agreement (Figure 5). The difference between measured and simulated Hg loads ranged from -28 to +1.2% for Hg_t and -5.0 to +3.7% for CH_3Hg loads. Annual load from Weber River to GSL during the monitoring period was 0.3 kg of Hg_t (Figure 3) and 7.8 g of CH_3Hg.

Kennecott Drain near Magna, Utah: The Kennecott Drain had only intermittent flows during the monitoring period (Figure 6) which did not allow for a sufficient number of water-quality samples to be collected for Hg load simulation using LOADEST. The two water-quality samples that were collected from the Kennecott Drain in October 2005 and May 2007 contained very low concentrations of Hg_t (1.8 and 1.4 ng/l) and CH_3Hg (< 0.04 and < 0.04 ng/l). An annual Hg load from the Kennecott Drain was estimated by assuming a constant Hg_t (1.4 ng/l) and CH_3Hg concentration during the annual monitoring period from April 1, 2007 through March 31, 2008. Since both of the CH_3Hg samples were below the method detection limit (MDL) of 0.04 ng/l, a concentration value of 0.75 times the MDL was used to estimate CH_3Hg concentration. The constant Hg concentration data was then combined with the mean daily discharge data during the same monitoring period to estimate annual loads. Annual Hg load from the Kennecott Drain to GSL during the monitoring period was extremely low (0.01 kg of Hg_t and 0.2 g of CH_3Hg) (Figure 3).

Figure 5–Stream discharge and dates when mercury samples were collected at the Weber River gaging station (A) and comparison between measured and modeled total mercury loads (B). Dashed line indicates one-to-one correspondence between measured and modeled mercury loads.

Bear River Bay Outflow at GSL Minerals Corp. Bridge: The LOADEST model calibration file contained seven observations for Hg_t and CH_3Hg during the time period of April 2007 through March 2008 (Figure 7). Because of equipment failure and seasonal gage removal due to ice conditions, daily discharge measurements for the time periods of March 1, 2007 through April 17, 2007 and July 5, 2007 through March 31, 2008 were not made. Instead discharge was estimated from an adjacent upstream gage (Bear River near Corinne, Utah). Mean daily discharge for the missing time period was estimated from the linear relationship between measured discharge at both sites from March 21, 2006 through September 30, 2006. The regression equation developed from this comparison explained 80% of the variance in discharge (p < 0.0001, N = 194) between the two gage sites. The LOADEST estimation file contained 397 actual and estimated measurements of mean daily discharge ranging from < 0.1 to 85.0 m^3/s during the time period from March 2007 through March 2008. Regression model 4 (Table 1) was determined to best simulate daily Hg_t loads ($R^2 = 0.9977$) and model 7 (Table 1) was determined to best simulate daily CH_3Hg loads ($R^2 = 0.9993$) from Bear River to GSL.
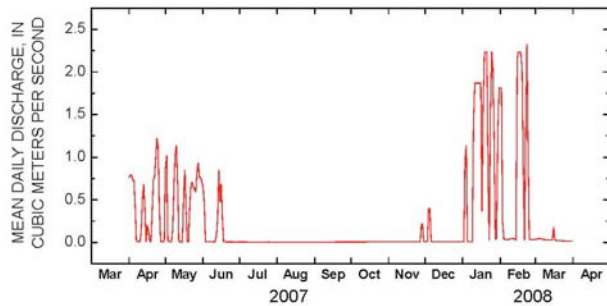

Figure 6–Discharge from the Kennecott Drain gaging station during April 1, 2007 through March 31, 2008.

During the periods of measurable discharge, agreement between the measured and simulated loads of Hg at the Bear River gage was good (Figure 7). The difference between measured and simulated Hg loads during measurable discharge ranged from -8.9 to +0.5% for Hg_t and +0.3 to +2.9% for CH_3Hg loads. Annual load from Bear River to GSL during the monitoring period was 2.2 kg of Hg_t (Figure 3) and 695 g of CH_3Hg.

Farmington Bay Outflow at Causeway Bridge: The LOADEST model calibration file contained seven observations for Hg_t and CH_3Hg during the time period of April 2007 through March 2008 (Figure 8). The LOADEST estimation file contained 397 measurements of mean daily discharge ranging from < 0.1 to 41 m^3/s during the time period from March 2007 through March 2008. Regression model 1 (Table 1) was determined to best simulate daily

Hg_t loads ($R^2 = 0.6771$) and model 4 (Table 1) was determined to best simulate daily CH_3Hg loads ($R^2 = 0.8597$) from Farmington Bay to GSL.

Measured and simulated loads of Hg_t at the Farmington Bay outflow gage are shown in Figure 8. Simulated total Hg loads did not consistently agree with measured loads. The difference between measured and simulated Hg loads ranged from -90.4 to +39.1% for Hg_t and -83.7 to +40.0% for CH_3Hg loads. Annual load from Farmington Bay to GSL during the monitoring period was 2.8 kg of Hg_t (Figure 3) and 330 g of CH_3Hg.
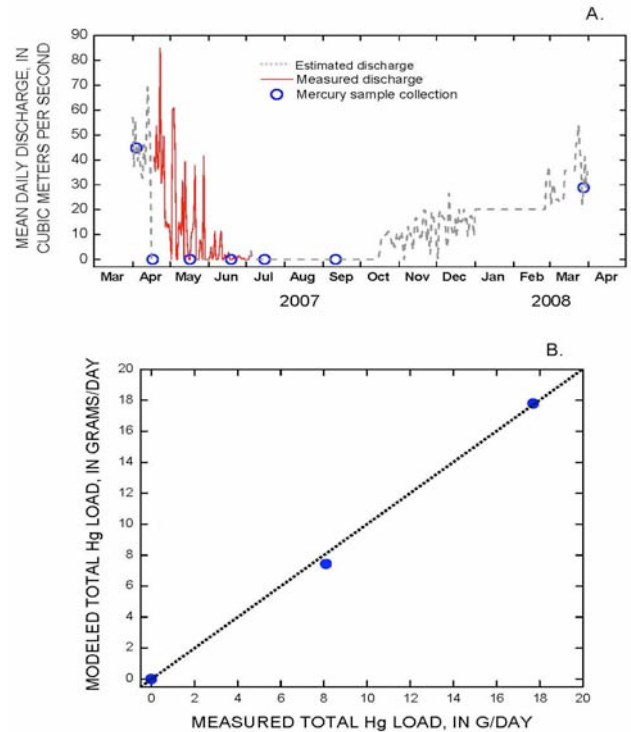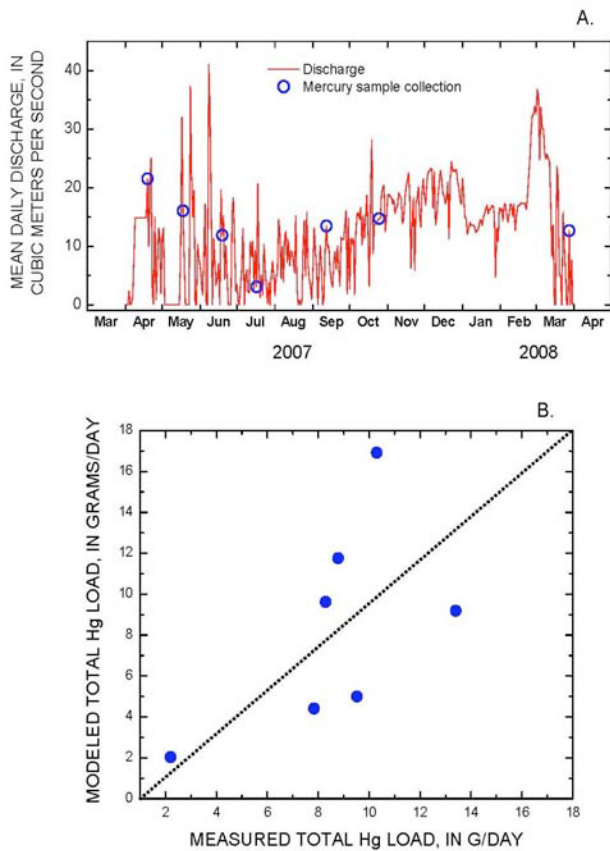

Figure 7–Stream discharge and dates when mercury samples were collected at the Bear River gaging station (A) and comparison between measured and modeled total mercury loads (B). Dashed line indicates one-to-one correspondence between measured and modeled mercury loads.

Cumulative Hg Loadings

The Hg input models developed for each gage site were used to estimate the cumulative total (dissolved + particulate) Hg_t load to GSL from April 2007 through March 2008 (Figure 3). Total estimated Hg_t load to GSL during this 1 year time period was 6 kg. Almost 50% of the annual Hg_t load was contributed by outflow from Farmington Bay (2.8 kg). The second major contributor of Hg_t to GSL was from the Bear River (36%). Minor Hg_t loads (< 18%) were contributed by the four remaining inflow sites (Goggin Drain, Lee Creek, Weber River, and KUCC outfall).

Figure 8–Stream discharge and dates when mercury samples were collected at the Farmington Bay outflow gaging station (A) and comparison between measured and modeled total mercury loads (B). Dashed line indicates one-to-one correspondence between measured and modeled mercury loads.

Bodaly et al. (1998) found that sewage treatment typically removes 88% of Hg_t from raw sewage, likely discounting this as a large source of additional Hg_t. Alternatively, Hg_t inputs from untreated urban sources such as stormwater runoff could contribute to the elevated Hg_t loads observed in the Farmington Bay drainage basin. Fulkerson et al. (2007) found that stormwater runoff from impervious surfaces (roads, parking lots, etc.) contained elevated concentration of Hg_t that was mostly derived from dry deposition. Approximately 85% of the particulate Hg_t was removed from impervious surfaces during rainfall events. In a similar study of urban runoff from impervious surfaces, Eckley & Branfireun (2008) found that the highest Hg_t concentration in runoff were observed during the rising limb of the hydrograph and was dominated by particulate bound Hg_t.

It is possible that the elevated Hg_t loads observed in the Farmington Bay outflow could be related to urban runoff within the drainage basin. Box plots showing the concentration of Hg_t in five of the six inflow sites to GSL indicates that inflow from Weber River had the highest median concentration of Hg_t, followed by inflow from Farmington Bay (Figure 9). The higher median discharge at the Farmington Bay inflow relative to Weber River accounts for the significantly higher annual Hg_t loads contributed to GSL from Farmington Bay. Additional study evaluating the transport, settling, and resuspension of particulate bound Hg_t derived from impervious surfaces would be an important component of future work.

It is also possible that the elevated Hg_t loads from Farmington Bay and Bear River Bay outflows could be partly related to atmospheric deposition directly on the water surface. Both gage sites have large surface areas of slow-moving water that could receive direct atmospheric deposition of Hg (Figure 1).

Table 1–Regression models considered during the automated selection option in LOADEST (Runkel et al. 2004). [a_0 thru a_6, model-determined regression coefficients; ln, natural log; Q, discharge; dtime, decimal time; pi, 3.141593].

Model Number	Regression Model
1	$a_0 + a_1 \ln Q$
2	$a_0 + a_1 \ln Q^2$
3	$a_0 + a_1 \ln Q + a_2 dtime$
4	$a_0 + a_1 \ln Q + a_2 \sin(2\pi dtime) + a_3 \cos(2\pi dtime)$
5	$a_0 + a_1 \ln Q + a_2 \ln Q^2 + a_3 dtime$
6	$a_0 + a_1 \ln Q + a_2 \ln Q^2 + a_3 \sin(2\pi dtime) + a_4 \cos(2\pi dtime)$
7	$a_0 + a_1 \ln Q + a_2 \sin(2\pi dtime) + a_3 \cos(2\pi dtime) + a_4 dtime$
8	$a_0 + a_1 \ln Q + a_2 \ln Q^2 + a_3 \sin(2\pi dtime) + a_4 \cos(2\pi dtime) + a_5 dtime$
9	$a_0 + a_1 \ln Q + a_2 \ln Q^2 + a_3 \sin(2\pi dtime) + a_4 \cos(2\pi dtime) + a_5 dtime + a_6 dtime^2$

43

Comparison of Atmospheric Deposition
of Hg to Riverine Loadings

Atmospheric deposition can be one of the major sources of Hg to aquatic environments (Krabbenhoft & Rickert 1995); therefore, determination of the relative proportions of riverine versus direct atmospheric Hg inputs to the lake surface of GSL will be important for understanding Hg cycling in the lake and developing future remediation strategies. Atmospheric Hg deposition can be from both dry and wet deposition directly to the surface of GSL. The surface area of GSL used in the atmospheric deposition calculations was calculated for the highest mean monthly lake elevation recorded at both the south (1279.4 m) and north arm (1279.2 m) of GSL during the spring of 2007. Based on lake area tables developed for GSL by Baskin (2005, 2006), a maximum lake surface area of 3.2×10^9 m^2 was available (not including Farmington or Bear River Bays) during the study period for atmospheric Hg deposition.

Measurements and associated modeling of dry deposition of reactive gaseous mercury (RGM) to the surface of GSL was conducted over a one year period (2006–2007) by Peterson & Gustin (2008). Annual dry deposition of Hg modeled by Peterson & Gustin (2008) was 4.4 $\mu g/m^2$. Using the cumulative surface area of GSL during the spring of 2007 of 3.2×10^9 m^2, approximately 14 kg of Hg would be deposited to the lake surface during 2006–2007.

Wet deposition of Hg to the surface of GSL was estimated using the newly installed Mercury Deposition Network (MDN) site located near GSL (Latitude: 40° 42' 42.48"; Longitude: 111° 57' 39.23"; Elevation: 1297 m). This MDN site has been operating since May 2007 and wet deposition Hg data currently (2008) exist for 13 months during May 2007 through May 2008 (Table 2) (National Atmospheric Deposition Program 2008). Wet deposition data collected during the 12 months from May 2007 through April 2008 resulted in a cumulative Hg deposition of 5.5 $\mu g/m^2$ (Table 2). Combining the cumulative surface area of GSL during the spring of 2007 of 3.2×10^9 m^2 with the estimated annual wet deposition value, approximately 18 kg of Hg would be deposited to GSL via wet deposition processes.

Comparison of annual cumulative atmospheric (32 kg) versus riverine (6 kg) deposition of Hg_t to GSL indicates that atmospheric deposition processes are the major input source to GSL by over 5:1. Additional atmospheric and riverine Hg data are needed to further confirm and refine these annual deposition amounts. The combined annual atmospheric and riverine input masses of Hg were compared to longer-term Hg deposition rates estimated from sediment records in GSL. These results are presented in the following section.

Table 2–Precipitation and mercury data collected from the Mercury Deposition Network monitoring site located near Great Salt Lake, Utah (site UT97) (National Atmospheric Deposition Program, 2008). [SVOL, sample volume; HgConc, total mercury concentration reported by the contract lab; HgDep, total mercury deposition; mm, millimeters; ml, milliliters; ng/l, nanograms per liter; ng/m^2, nanograms per square meter]

| Month and Year	SVOL, ml	HgConc, ng/l	HgDep, ng/m^2
May 2007	75.0	28.50	131.1
June 2007	112.1	39.60	764.3
July 2007	185.5	67.90	286.2
August 2007	61.7	46.80	454.0
September 2007	238.9	80.50	444.9
October 2007	328.8	48.80	896.8
November 2007	159.0	22.30	103.5
December 2007	314.8	16.50	450.7
January 2008	255.3	40.90	360.5
February 2008	261.0	22.70	329.1
March 2008	279.0	36.20	355.3
April 2008	321.4	309.90	938.2
May 2008	218.9	96.30	671.0

Sediment-Core Records of Cumulative Hg Inputs

The upper 10 cm section of a sediment core collected from site 3510 (Figure 1) during 2006 was used as a proxy record to reconstruct long-term records of Hg_t deposition in GSL. Sediment accumulation rates (g/cm^2.yr) were determined from ^{210}Pb and ^7Be profiles versus cumulative mass instead of depth to account for sediment compaction.

The ^{210}Pb activity decreases with increasing depth in sediment to the supported activity defined by ^{226}Ra at the 10 cm depth (Figure 10). The decrease in unsupported activity was exponential as illustrated by plotting the natural log of unsupported ^{210}Pb versus cumulative sediment mass (Figure 10), resulting from decay of the unsupported ^{210}Pb activity over time by its characteristic decay rate with a half life of 22.3 years (Bierman et al. 1998). Unsupported ^{210}Pb results from emanation of ^{222}Rn from continental land masses, decay in the atmosphere to ^{210}Pb, and subsequent deposition onto the lake surface and watershed, followed by scavenging to sediment particles and/or erosion from the watershed that are subsequently deposited on the lake bed. The zone of near constant ^{210}Pb activity between 0 and 3 cm may reflect a period of

increased accumulation or mixing of the sediment due to physical processes, such as episodic resuspension and redeposition of surface sediments during wind events (Beisner et al. 2008). Biological mixing of sediments is unlikely because of the anoxic conditions in the DBL.
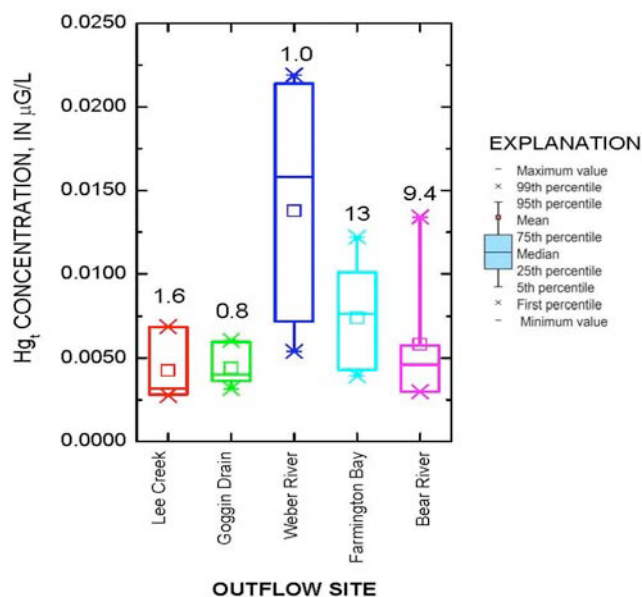
Figure 9–Box plots of whole water Hg_t concentration in water samples from selected inflow sites to Great Salt Lake compared to median daily discharge in m^3/s during April 1, 2007 through March 31, 2008. With the exception of Bear River, analytical results from seven water samples were used for each box plot. Data from six water-quality samples were used for Bear River.

The presence of ^7Be in the top 2 cm (Figure 11) is consistent with rapid deposition of sediments. The source of ^7Be is atmospheric deposition to the lake surface and rapid scavenging to suspended particulate material. Because of its 53 day half life, the ^7Be in the 1-2 cm depth interval can only occur if some fraction of the sediment was in the water column within the past 200 days to accumulate ^7Be. The presence of ^7Be is likely the result of non-biological resuspension and redeposition processes in GSL.

Sediment mass accumulation rate (MAR) was determined from the ^{210}Pb profile using the constant flux–constant sedimentation rate, CF-CS, method (Appleby & Oldfield 1992). The CF-CS method assumes a steady state accumulation of sediments and a constant unsupported ^{210}Pb activity per gram of depositing sediment particles. The sediment mass accumulation rate ($g/cm^2.yr$) was calculated from the slope of the linear regression of the ln (unsupported ^{210}Pb, dpm/g dry sediment) versus the cumulative dry mass, g/cm^2 from 2.5 to 9.5 cm (Figure 10). The core profile was well described by a single regression ($R^2 = 0.98$) yielding an overall MAR of 0.044 $g/cm^2.yr$

(Figure 10). The age of the midpoint of each sediment interval was then calculated by dividing the cumulative mass (g/cm^2) at the middle of each depth interval by the overall MAR, and subtracted from the core collection date to assign a calendar year for each interval. The resulting dates are depicted on Figure 11. These dates do not account for the processes affecting the upper 3 cm of the sediment profile. To correct for processes that resulted in the zone of constant ^{210}Pb activity (0 to 3 cm interval) and the presence of ^7Be (0 to 2 cm), the sediment ages were recalculated starting at 2 cm and assuming the 0-2 cm sediment horizon is < 1 year of age. Sediment chronologies are shown as a function of depth in Figure 11 with and without the 2 cm active layer. The effect of accounting for the 2 cm active layer in deriving the sediment chronology is a shift in sediment age to about 5 years younger in each interval below the active layer. This approach assumes that sediments below 2 cm in depth are no longer available for resuspension and are effectively preserved.

The chronology of the sediment core was then combined with the salt corrected Hg_t concentration determined from each 1 cm section to calculate annual Hg_t deposition rates (Table 3). Based on the sediment record collected from site 3510, the mean annual Hg_t deposition ranged from 55 to 150 $\mu g/m^2$. These reconstructed annual deposition amounts are significantly higher than the combined dry deposition (4.4 $\mu g/m^2.yr$) (Peterson & Gustin 2008) and wet deposition (5.5 $\mu g/m^2.yr$) estimated for GSL. Uniform distribution of riverine Hg_t discharge over the cumulative 2007 surface area of GSL (3.2 x 10^9 m^2) would add another 1.9 $\mu g/m^2.yr$ of Hg_t, resulting in a cumulative annual atmospheric plus riverine deposition of 11.8 $\mu g/m^2$.

The large difference between the cumulative measured Hg_t deposition (11.8 $\mu g/m^2.yr$) and reconstructed Hg_t deposition (average = 130 $\mu g/m^2.yr$) over the last ~ 100 years from the site 3510 sediment core is likely the result of sediment focusing in GSL. Sediment focusing is the preferential deposition of sediments and associated contaminants at a site from both the redistribution of sediments from within the lake and from sediments delivered from the watershed (Van Metre et al. 1997). Previous studies have found that uniform sedimentation is not present throughout the south arm of GSL. Colman et al. (2002) mapped post-Bonneville sediment thickness in the South Arm of GSL and found large variations in sediment thickness ranging from < 2 m to 10 m with a thickness of 5 to 6 m at site 3510. Oliver et al. (in review) used ^{210}Pb profiles of shallow sediment cores collected from the South Arm of GSL to investigate

sedimentation rates over the past ~ 100 years. The ^{210}Pb profiles indicated a wide range of sedimentation mass accumulation rates (MARs) from near 0.00 g/cm^2.yr (with no detectable unsupported ^{210}Pb) to areas with MARs up to 0.05 g/cm^2.yr. These MARs translate into compacted linear sedimentation rates ranging from 0.00 to 0.08 cm/yr, with site 3510 near the upper end of the range at 0.05 cm/yr. Thus, the high annual Hg deposition rates determined in the sediment core from site 3510 are likely the result of sediment focusing in GSL to this site. Mercury concentration in additional sediment cores collected from other areas of GSL are needed to further refine lake-wide rates of cumulative Hg$_t$ deposition. In addition, a measured atmospheric deposition rate for ^{210}Pb would provide a means to correct for sediment focusing to the core site.
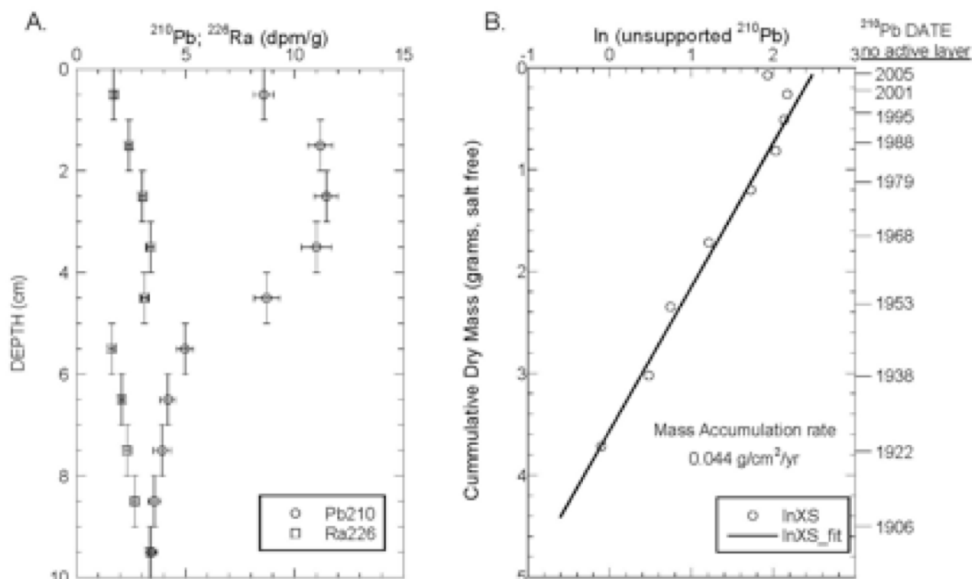
Figure 10–Total ^{210}Pb and ^{226}Ra activity, in disintegrations per minute per gram, versus depth in sediment core (A). Horizontal error bars depict 1 sigma uncertainty in measured activity based on counting statistics. Natural logarithm of unsupported ^{210}Pb activity versus cumulative dry sediment mass (B). Only data with measurable unsupported ^{210}Pb are presented. Solid line represents linear regression of the data used to derive sediment mass accumulation rate.
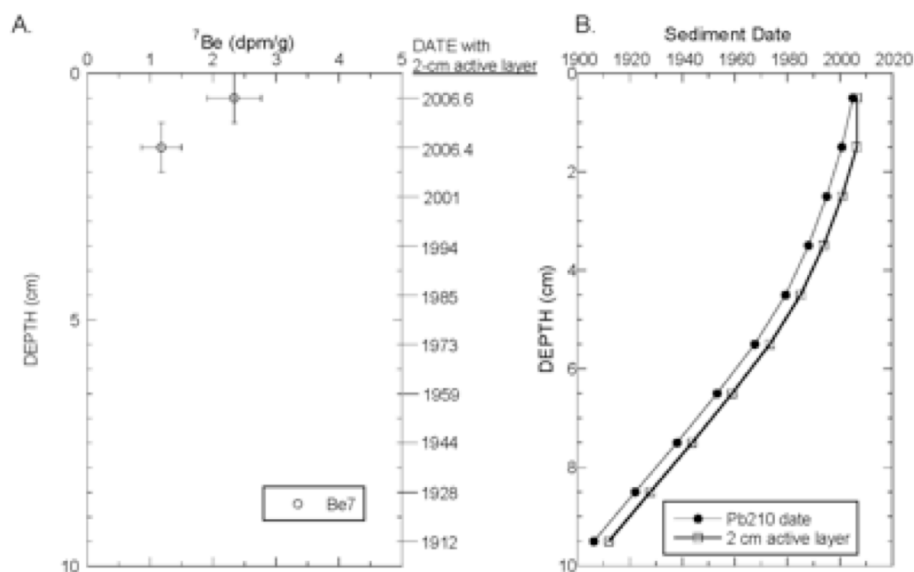
Figure 11–(A) ^{7}Be activity, in disintegrations per minute per gram, versus depth in sediment core. Horizontal error bars depict 1 sigma uncertainty in measured activity based on counting statistics. (B) Sediment deposition date as function of depth based on the sediment mass accumulations estimated from ^{210}Pb using the CF-CS method, with and without correction for 2 cm active layer. Non-linearity in deposition date versus depth is the result of sediment compaction.
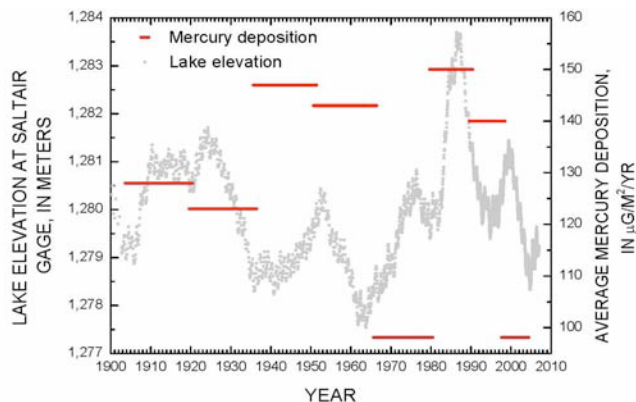
Figure 12–Comparison between historic lake elevation and reconstructed deposition rates of mercury using data collected from sediment core 3510. Because of resuspension processes, the deposition rates for the top 2 cm active layer were not plotted.

In addition to sediment focusing, the sediment core deposition rates show relatively large variations over the past ~ 100 years (Table 3). Historic changes in the lake elevation and resulting surface area of GSL could have a large effect on the total mass of Hg_t directly deposited onto GSL. As previously discussed, atmospheric deposition is estimated to contribute about 84% of the current Hg to GSL, with riverine inputs comprising the remaining 16%. Unlike most freshwater lakes, small changes in lake elevation results in large changes in the surface area "footprint" of GSL that is available to receive Hg inputs via direct atmospheric deposition (Baskin 2005, 2006). With this process in mind, historic changes in the Hg_t deposition rates recorded in the sediment core from site 3510 were compared to changes in lake elevation in the South Arm of GSL (Figure 12).

During the past ~ 60 years, there is very good agreement between lake elevation and Hg_t deposition (Figure 12). The highest Hg_t deposition rate recorded in the sediment core (> 150 μg/m^2.yr) corresponds to the highest lake level of GSL in recent history. In contrast, the lowest Hg_t deposition rate recorded in the sediment core (< 100 μg/m^2.yr) is in close correspondence with one of the lowest lake levels of GSL in recent history.

During the mid-1930s to the early 1950s the lake level was low; however, there is a relatively high Hg_t deposition rate (~ 147 μg/m^2.yr) recorded in the sediment core (Figure 12). This high Hg_t deposition combined with a low lake elevation could reflect a period of higher global anthropogenic inputs of atmospheric Hg from increased industrial output related to World War II. An ice core collected in northwestern Wyoming (330 km northeast of GSL) showed a spike in Hg_t concentration in ice samples corresponding to snow deposited in the early to mid-1940s (Figure 13). Furthermore, global Hg production also shows a large spike during this same time period (Figure 13).

Based on these initial sediment core results, high lake levels and resulting increased surface area, combined with sediment focusing processes may increase Hg_t accumulation rates in sediment in specific areas of GSL.
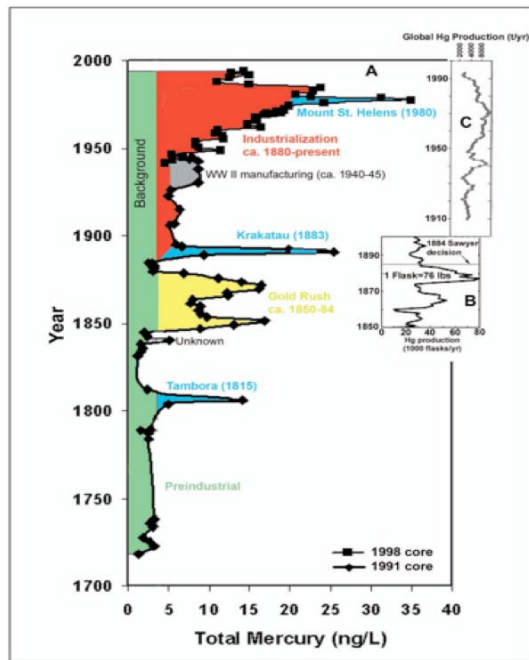
Figure 13–(A) Profile of historic concentrations of Hgt in the Upper Fremont Glacier (used with permission from Schuster et al. 2002). A conservative concentration of 4 ng/l was estimated as preindustrial inputs and extrapolated to 1993 as a background concentration. Age-depth prediction limits are (10 years (90% confidence level); confidence limits are 2–3 years. (Inset B) Hg production during the California Gold Rush (Alpers & Hunerlach 2000). (Inset C) World production of Hg in tons per year during the last century (Engstrom & Swain 1997).

SUMMARY

Despite the ecological and economic importance of GSL, little is known about current and historic Hg inputs to the lake. Regression modeling techniques were used to estimate whole-water Hg_t and CH_3Hg loads to GSL from six major inflow sources during a one-year period from April 1, 2007 to March 31, 2008. Annual Hg_t loads to GSL ranged from 0.01 kg (KUCC outfall) to 2.8 kg (Farmington Bay outflow). Cumulative Hg_t load to GSL during this 1 year time period was 6 kg, with almost 50% of the cumulative Hg_t load contributed by outflow from Farmington Bay. According to previous research, urban runoff from impervious surfaces in the Farmington Bay watershed, which includes Salt Lake City, may be responsible for the high proportion of Hg_t inputs from Farmington Bay and should be a component of future studies.

Dry deposition of Hg measured by Peterson and Gustin (2008) was combined with the 2007 maximum surface area of GSL to estimate a cumulative dry depositon rate of 14 kg/yr. Cumulative wet depositon of Hg to the surface of

GSL was estimated to be 18 kg/yr using data collected at the MDN site near GSL (National Atmospheric Deposition Program 2008). Comparison of cummulative annual atmosphereic Hg deposition (32 kg) to annual riverine input (6 kg) indicates that atmospheric deposition is the dominant input source to GSL. A sediment core collected from the southern arm of GSL was used to reconstruct annual Hg_t deposition rates over the past $\sim$ 100 years. The large difference between the reconstructed Hg_t deposition from the sediment core (average = 130 $\mu g/m^2$.yr) to the cumulative measured Hg_t deposition (riverine + atmospheric) of 11.8 $\mu g/m^2$.yr is likely the result of focusing of sediment to this site in GSL. Unlike most freshwater lakes, small changes in water level in GSL significantly changes the lake surface area available for direct deposition of atmospheric Hg. There is good agreement between lake elevation (and corresponding lake surface area) and Hg_t deposition rates estimated from the sediment core over the past 60 years. Changes in lake surface area during historic lake-level flucuations combined with sediment focusing processes are proposed to explain the reconstructed variations in Hg_t deposition rates from the sediment core collected from GSL.

Table 3–Mean annual total mercury deposition in Great Salt Lake from 1904 to 2006 using sediment-core data from site 3510. Year of sediment deposition was determined using the 2 cm active layer model.

Sample interval, in cm	Year(s) of deposition	Salt-corrected total Hg concentration, in $\mu g/g$	Mean annual Hg deposition, in $\mu g/m^2$
0 to 2	2004 to 2006	*0.126	55.4
2 to 3	1998 to 2004	0.223	98.1
3 to 4	1990 to 1998	0.319	140.0
4 to 5	1980 to 1990	0.340	150.0
5 to 6	1966 to 1980	0.223	98.1
6 to 7	1951 to 1966	0.326	143.0
7 to 8	1936 to 1951	0.335	147.0
8 to 9	1920 to 1936	0.279	123.0
9 to 10	1904 to 1920	0.290	128.0

*Average concentration from two samples (0-1 and 1-2 cm)

ACKNOWLEDGEMENTS

REFERENCES

Aldrich, T.W. & D.S. Paul. 2002. Avian ecology of Great Salt Lake. In: Gwynn, J.W. (ed), Great Salt Lake: An Overview of Change. Utah Department of Natural Resources Special Publication: 343–374.

Alpers, C.N. & M.P. Hunerlach. 2000. Mercury contamination from historic gold mining in California. U.S. Geological Survey Fact Sheet 0061-00: 6 p.

Anderson, C.D. & V. Anderson. 2002. Nutritional enterprises on Great Salt Lake-North Shore Limited Partnership and Mineral Resources International. In: Gwynn, J.W. (ed), Great Salt Lake: An Overview of Change. Utah Department of Natural Resources Special Publication: 235–241.

Appleby, P.G. & F. Oldfield. 1992. Application of ^{210}Pb to sedimentation studies. In: Ivanovich, M. & R.S. Harmon (eds), Uranium-series Disequilibrium: Application to Earth, Marine, and Environmental Sciences, Second edition, Clarendon Press, Oxford: 731–778.

Baskin, R.L. 2005. Calculation of area and volume for the south part of Great Salt Lake, Utah. U.S. Geological Survey Open-File Report 2005-1327: 6 p.

Baskin, R.L. 2006, Calculation of area and volume for the north part of Great Salt Lake, Utah: U.S. Geological Survey Open-File Report 2006-1359, 6 p.

Baskin, R.L. & D.V. Allen. 2005. Bathymetric map of the south part of Great Salt Lake, Utah. U.S. Geological Survey Scientific Investigations Map 2894.

Beisner, K., D.L. Naftz & W.P. Johnson. 2008. Evidence and implications of movement of the Deep Brine Layer the South Arm of Great Salt Lake, Utah. This volume.

Bierman, P.R., A. Albrecht, M.H. Bothner, E.T. Brown, T.D. Bullen, L.B. Gray, & L. Turpin. 1998. Erosion, weathering, and sedimentation L. In: Kendall, C. and J.J. McDonnell (eds), Isotope Tracers in Catchment Hydrology. Elsevier, Amsterdam: 647–678.

Bodaly, R.A., W.M. Rudd & R.J. Flett. 1998. Effect of urban sewage treatment on total and methyl mercury concentrations effluents. Biogeochemistry 40: 279–291.

Buchanan, T.J. & W.P. Somers. 1968. Stage measurements at gaging stations. In: U.S. Geological Survey Techniques of Water-Resources Investigations, Book 3, Ch. A7: 28 p.

Buchanan, T.J. & W.P. Somers. 1969. Discharge measurements at gaging stations. In: U.S. Geological Survey Techniques of Water-Resources Investigations, Book 3, Ch. A8: 65 p.

Butts, D. 2002. IMC Kalium Ogden Corporation-Extraction of non-metals from Great Salt Lake. In: Gwynn, J.W. (ed), Great Salt Lake: An Overview of Change. Utah Department of Natural Resources Special Publication: 227–233.

Carter, R.W. & J. Davidian. 1968. General procedure for gaging streams. In: U.S. Geological Survey Techniques of Water-Resources Investigations, Book 3, Ch. A6: 13 p.

Cohn, T.A. 1988. Adjusted maximum likelihood estimation of the moments of lognormal populations from type I censored samples. U.S. Geological Survey Open-File Report 88-350: 34 p.

Cohn, T.A., E.J. Gilroy & W.G. Baier. 1992. Estimating fluvial transport of trace constituents using a regression model with data subject to censoring. In: Proceedings of the Joint Statistical Meeting, Boston, MA: 42–151.

Colman, S.M., K.R. Kelts & D.A. Dinter. 2002. Depositional history and neotectonics in Great Salt Lake, Utah, from high-resolution seismic stratigraphy. Sedimentary Geology 148: 61–78.

Cutshall, N.H., I.L. Larsen & C.R. Olsen. 1983. Direct analysis of ^{210}Pb in sediment samples: Self-absorption corrections. Nuclear Instruments and Methods 306: 309–312.

DeWild, J.F., M.L. Olson & S.D. Olund. 2002. Determination of methyl mercury by aqueous phase ethylation, followed by gas chromatographic separation with cold vapor atomic fluorescence detection. U.S. Geological Survey Open-File Report 01-445: 14 p.

Eckley, C.S. & B. Branfireun. 2008. Mercury mobilization in urban stormwater runoff. Science of the Total Environment. 403: 164–167.

Engstrom, D.R. & E.B. Swain. 1997. Recent declines in atmospheric mercury deposition in the Upper Midwest. Environmental Science and Technology 31: 960–967.

Fulkerson, M., F.N. Nnadi & L.S. Chasar. 2007. Characterizing dry deposition of mercury in urban runoff. Water, Air, & Soil Pollution 185: 21–32.

Fuller, C.C., A. vanGeen, M. Baskaran & R. Anima. 1999. Sediment chronology in San Francisco Bay defined by ^{210}Pb, ^{234}Th, ^{137}Cs, and ^{239,240}Pu. Marine Chemistry 64: 7–27.

Isaacson, A.E., F.C. Hachman & R.T. Robson. 2002. The economics of Great Salt Lake, In: Gwynn, J.W. (ed), Great Salt Lake: An Overview of Change. Utah Dept. of Natural Resources Special Publication: 187–200.

Judge, G.G., R.C. Hill, W.E. Griffiths, H. Lutkepohl & T.C. Lee. 1988. Introduction to theory and practice of econometrics (2nd ed.). John Wiley, New York: 1024 p.

Krabbenhoft, D.P. & D.A. Rickert. 1995. Mercury contamination of aquatic ecosystems. U.S. Geological Survey Fact Sheet 216-95.

Loving, B.L., K.M. Waddell & C.W. Miller. 2000. Water and salt balance of Great Salt Lake, Utah, and simulation of water and salt movement through the causeway, 1987–98. U.S. Geological Survey Water-Resources Investigations Report 00-4221.

Naftz, D.L., B. Waddell, N. Darnall, C. Perschon & J. Garbarino. 2006. Great Salt Lake, United States: Evidence of anthropogenic pressures to the fourth largest terminal lake in the world. Geophysical Research Abstracts, Vol. 8, European Geosciences Union Annual Meeting, April 2006, Vienna, Austria.

Naftz, D.L., C. Angeroth, T. Kenney, B. Waddell, S. Silva, N. Darnall, C. Perschon & J. Whitehead. 2008. Anthropogenic influences on the input and biogeochemical cycling of nutrients and mercury in Great Salt Lake, Utah, USA. Applied Geochemistry 23: 1731–1744.

National Atmospheric Deposition Program. 2008. Data available for NADP/MDN Site: UT97 (Salt Lake City), http://nadp.sws.uiuc.edu/nadpdata/mdnRequest.asp?site=UT97. Accessed 16 July 2008.

Oliver, W., D.L. Naftz, W.P. Johnson, X. Diaz, and C. Fuller. in review. Estimating selenium removal by sedimentation from the Great Salt Lake, Utah. Applied Geochemistry.

Olson, M.L. & J.F. DeWild. 1999. Techniques for the collection and species specific analysis of low levels of mercury in water, sediment, and biota. U.S. Geological Survey Water-Resources Investigation Report 99-4018-B: 11 p.

Olund, S.D., J.F. DeWild, M.L. Olson & M.T. Tate. 2004. Methods for the preparation and analysis of solids and suspended solids for total mercury. U.S. Geological Survey Techniques and Methods Report 5-A8: 23 p.

Peterson, C. & M.S. Gustin. 2008. Mercury in the air, water and biota at the Great Salt Lake (Utah, USA). Science of the Total Environment 405: 255–268.

Runkel, R.L., C.G. Crawford & T.A. Cohn. 2004. Load estimator (LOADEST): A FORTRAN Program for estimating constituent loads in streams and rivers. In: U.S. Geological Survey Techniques and Methods Book 4, Ch. A5: 69 p.

Schuster, P.F., D.P. Krabbenhoft, D.L. Naftz, L.D. Cecil, M.D. Olson, J.F. DeWild, D.D. Susong & J.R. Green. 2002. Atmospheric mercury deposition during the last 270 years: A glacial ice core of natural and anthropogenic sources. Environmental Science and Technology 36: 2303–2310.

Simpson, M.R. 2001. Discharge measurements using a broad-band acoustic Doppler current profiler. U.S. Geological Survey Open-File Report 01-1: 123 p.

Tripp, G.T. 2002. Production of magnesium from the Great Salt Lake. In: Gwynn, J.W. (ed), Great Salt Lake: An Overview of Change. Utah Department of Natural Resources Special Publication: 221–225.

U.S. Environmental Protection Agency. 2000. Guidance for assessing chemical contaminant data for use in fish advisories, vol. 1. Fish Sampling and Analysis, third ed., USEPA Report EPA 823-B-00-007.

Utah Department of Health. 2005. An evaluation of mercury concentrations in waterfowl from the Great Salt Lake, Utah for 2004 and 2005. Health Consultation Report.

Van Metre, P.C., E. Callender & C.C. Fuller. 1997. Historical trends in organochlorine compounds in river basins identified using sediment cores from reservoirs. Environmental Science and Technology 31: 2339–2344

Van Metre, P.C., J.T. Wilson, C.C. Fuller, E. Callender & B.J. Mahler. 2004. Collection, analysis, and age-dating of sediment cores from 56 U.S. lakes and reservoirs sampled by the U.S. Geological Survey, 1992–2001. U.S. Geological Survey Scientific Investigations Report 2004-5184.

Van Metre, P.C., A.J. Horowitz, B.J., Mahler, W.T. Foreman, C.C. Fuller, M.R. Burkhardt, K.A. Elrick, E.T. Furlong, S. Skrobialowski, J.J. Smith, J.T. Wilson & S.D. Zaugg. 2006. The impact of hurricanes Katrina and Rita on the chemistry of bottom sediments in Lake Pontchartrain, Louisiana, USA. Environmental Science and Technology 40: 6895–6902.